# Selected Topics on Hadronic $B$ Decays from BaBar

K. Suzuki[a]

[a]Stanford Linear Accelerator Center,
MS 62, 2575 Sand Hill Road, Menlo Park, CA 94304, USA

Recent measurements of branching fractions and decay-rate asymmetries in charmless hadronic $B$ decays at the BaBar experiment are presented. The selected topics include Dalitz plot analyses of $B \to K^+\pi^-\pi$ and signal searches in $B \to PP$ and $PV$, where isoscalar mesons are involved, and in $B \to b_1 P$; $P$ and $V$ denote a pseudoscalar and vector meson, respectively. Several measurements in charmless hadronic $B$ decays have indicated possible deviations from the theoretical predictions within the Standard Model. The measurements presented would contribute to searching for and resolving such puzzles.

## 1. INTRODUCTION

### 1.1. Charmless hadronic $B$ decays

Charmless hadronic $B$ decays are dominated by $b \to u$ tree and $b \to s$ one-loop "penguin" transitions, shown in Fig. 1. The tree transitions involve $V_{ub}$, which is an element of the Cabibbo-Kobayashi-Maskawa (CKM) matrix [1], and information on the CKM angle $\gamma = \arg(V_{ub})$ may be accessible through these transitions. No weak phase is expected in the penguin transitions within the Standard Model (SM). The loop, however, may incorporate a contribution from new physics beyond the SM, which would deviate measurements from the SM predictions. Existence of the tree and the penguin amplitudes in a single decay may cause direct $CP$ violation due to their interference, giving a decay-rate asymmetry:

$$\mathcal{A}_{CP} \equiv \frac{\Gamma(\overline{f}) - \Gamma(f)}{\Gamma(\overline{f}) + \Gamma(f)} = \frac{2r\sin\delta\sin\gamma}{1 + 2r\cos\delta\cos\gamma + r^2}.$$

Here, $\Gamma(f)$ and $\Gamma(\overline{f})$ denote the decay widths of $B \to f$ and its charge conjugate decay $\overline{B} \to \overline{f}$, $r$ denotes the magnitude of the tree-to-penguin amplitude ratio, and $\delta$ denotes the strong phase difference between the two amplitudes; the weak phase difference results in $\gamma$ within the SM.

Absence of the CKM-favored $b \to c$ transition makes possible to access the CKM-suppressed and one-looped rare decays that are excellent processes to test the SM and to probe new physics. Hadronic uncertainty is always the issue in the theoretical predictions, and inputs from measurements are necessary to reduce the uncertainty. Systematic measurements of branching fraction ($\mathcal{B}$) and $\mathcal{A}_{CP}$ in various decays are important to improve theoretical understanding.

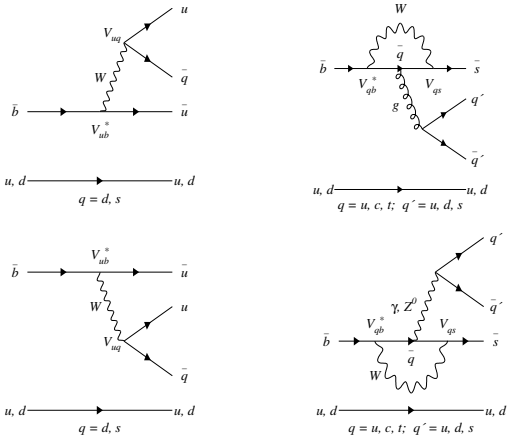


Figure 1. Feynman diagrams of color-allowed tree (upper left), gluonic penguin (upper right), color-suppressed tree (lower left) and electroweak penguin (upper right).

### 1.2. Puzzles – hints of new physics? –

Several measurements in charmless hadronic $B$ decays have indicated (possible) deviations from the SM predictions. One of such deviations is seen in the difference between $\mathcal{A}_{CP}$ in $B^0 \to K^+\pi^-$ and that in $B^+ \to K^+\pi^0$:

$\Delta\mathcal{A}_{CP}(K\pi) = \mathcal{A}_{CP}(K^+\pi^0) - \mathcal{A}_{CP}(K^+\pi^-)$. It is expected to be nearly zero in the SM while measurements show deviations [2,3]. This is referred as to "$\Delta\mathcal{A}_{CP}(K\pi)$ puzzle" and indicates unexpected enhancements of the color-suppressed tree and/or the electroweak penguin amplitudes; both only exist in $B^+ \to K^+\pi^0$.

Possible deviations from the SM predictions are seen in the difference between the $CP$-violating parameter $S$ in $b \to c\overline{c}s$ transition ($S_{c\overline{c}s}$) and that in $b \to s\overline{q}q$ transitions ($S_{s\overline{q}q}$; $q = d$ or $s$): $\Delta S = S_{s\overline{q}q} - S_{c\overline{c}s}$. It is expected to be nearly zero in the SM with slight positive deviations depending on decays, while measurements show slight negative deviations systematically [4]. This is referred as to "$\Delta S$ puzzle" and may indicate unexpected contributions through the loop in $b \to s\overline{q}q$ transitions.

Possible deviations are also seen in $B \to VV$ decays, referred as to "polarization puzzle", and is discussed in detail in Gao's talk [5]. These puzzles might be hints of new physics through the penguin loop. There might be more puzzles. Searching for and resolving such puzzles plays an important role in heavy-flavor physics.

## 2. GENERAL ANALYSIS PROCEDURE

The results presented are based on data produced with the PEP-II asymmetric-energy $e^+e^-$ storage rings [6] at SLAC and collected with the BaBar detector [7]. The data is taken at the $\Upsilon(4S)$ resonance with the $e^+e^-$ center-of-mass (CM) energy of $\sqrt{s} = 10.58$ GeV. Equal rates are assumed for the $B^0\overline{B}^0$ and $B^+B^-$ productions from $\Upsilon(4S)$. Throughout this proceeding, inclusion of charge conjugate decays is implied unless otherwise stated.

Analysis details can be found in the references given later for each analysis. General analysis procedure is as follows. Signal $B$ candidates are selected based on the two kinematic variables, $m_{\rm ES} = \sqrt{s/4 - p_B^{*2}}$ and $\Delta E = E_B^* - \sqrt{s}/2$, where $E_B^*$ and $p_B^*$ denote the energy and momentum, respectively, of a reconstructed $B$ candidate in the CM frame. The $m_{\rm ES}$ resolution is typically 3.0 MeV/$c^2$ while that of $\Delta E$ ranges in $20-50$ MeV depending on the decays, giving decay-dependent

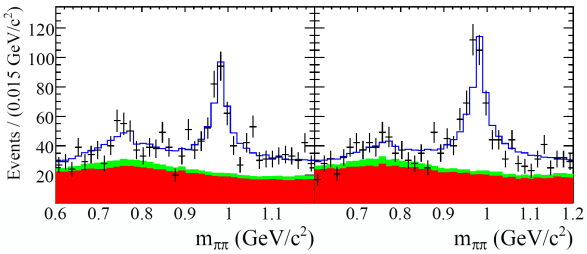


Figure 2. Dalitz plot fit projections for the candidates of $B^+ \to K^+\pi^-\pi^+$ (right) and of its charge conjugate decay (left) on the $\pi^+\pi^-$ invariant mass in the region of $\rho(770)^0$ and $f_0(980)$ [9]. Fit components are shown as the open, light-hatched and dark-hatched histograms for the total, misreconstructed $B$ decays, and $q\overline{q}$ background, respectively; they are superimposed on the data points, shown with error bars.

signal regions as areas in $m_{\rm ES} > 5.27$ GeV/c$^2$ and $|\Delta E| < 0.1-0.2$ GeV. Slight modifications on the kinematic variables are made in some analyses.

Dominant background arises from $e^+e^- \to q\overline{q}$ ($q = u$, $d$, $s$ or $c$) process, which is discriminated from the signal by utilizing event topology, angular correlations and an output of the $b$-flavor tagging algorithm [8]. Discrimination variables are combined into a single output of a multi-variate analyzer.

An unbinned extended maximum-likelihood fit is used to extract decay properties. A fit sample consists of signal, $q\overline{q}$ background and misreconstructed $B$ decays, over which likelihoods are summed up. A likelihood is evaluated from the product of probability density functions for $m_{\rm ES}$, $\Delta E$, the output of a multi-variate analyzer, and the event density over a Dalitz plot, in the Dalitz plot analyses, or resonance masses and helicity angles, in the analyses of (quasi-)two-body $B$ decays, where they are applicable.

## 3. DALITZ PLOT ANALYSES

### 3.1. Decay of $B^+ \to K^+\pi^-\pi^+$

As an effort to resolve the $\Delta\mathcal{A}_{CP}(K\pi)$ puzzle, it is important to measure $\mathcal{A}_{CP}$ in decays that have similar decay topology with $B^+ \to K^+\pi^0$. One of such decays is $B^+ \to \rho(770)^0K^+$, where a Dalitz plot analysis of the $K^+\pi^-\pi^+$ final state is

Table 1
Results obtained in the Dalitz plot analyses of $B^+ \to K^+\pi^-\pi^+$ [9] (upper rows) and $B^0 \to K^+\pi^-\pi^0$ [14] (lower rows). The first and second errors are statistical and systematic, respectively. The third error in the upper rows are the uncertainty on the isobar model. In the lower rows, the model uncertainty is included in the systematic error, and the third error addresses the wide spread of the multiple fit solutions for $(K\pi)^*_0$. Statistical significance of direct $CP$ violation is shown in the parenthesis of the last column if available. Note that the $\mathcal{B}$ results are not corrected for sub-decay branching fractions.

| Isobar component | Fit fraction [%] | $\mathcal{B}$ $[10^{-6}]$ | $\mathcal{A}_{CP}$ |
|---|---|---|---|
| $B^+ \to K^+\pi^-\pi^+$ (total) | — | $54.4 \pm 1.1 \pm 4.5 \pm 0.7$ | $+0.028 \pm 0.020 \pm 0.020 \pm 0.012$ |
| Non-resonant | $4.5 \pm 0.9 \pm 2.4 \,^{+0.6}_{-1.5}$ | $2.4 \pm 0.5 \pm 1.3 \,^{+0.3}_{-0.8}$ | — |
| $(K\pi)^{*0}_0\pi^+$ | $45.0 \pm 1.4 \pm 1.2 \,^{+12.9}_{-0.2}$ | $24.5 \pm 0.9 \pm 2.1 \,^{+7.0}_{-1.1}$ | $+0.032 \pm 0.035 \pm 0.020 \,^{+0.027}_{-0.019}$ $(1.2\sigma)$ |
| $K^*(892)^0\pi^+$ | $13.3 \pm 0.7 \pm 0.7 \,^{+0.4}_{-0.9}$ | $7.2 \pm 0.4 \pm 0.7 \,^{+0.3}_{-0.5}$ | $+0.032 \pm 0.052 \pm 0.011 \,^{+0.012}_{-0.007}$ $(0.9\sigma)$ |
| $K^*_2(1430)^0\pi^+$ | $3.40 \pm 0.75 \pm 0.42 \,^{+0.99}_{-0.13}$ | $1.85 \pm 0.41 \pm 0.28 \,^{+0.54}_{-0.08}$ | $+0.05 \pm 0.23 \pm 0.04 \,^{+0.18}_{-0.07}$ $(0.2\sigma)$ |
| $f_0(980)K^+$ | $18.9 \pm 0.9 \pm 1.7 \,^{+2.8}_{-0.6}$ | $10.3 \pm 0.5 \pm 1.3 \,^{+1.5}_{-0.4}$ | $-0.106 \pm 0.050 \pm 0.011 \,^{+0.034}_{-0.010}$ $(1.8\sigma)$ |
| $f_X(1300)K^+$ | $1.33 \pm 0.38 \pm 0.86 \,^{+0.04}_{-0.14}$ | $0.73 \pm 0.21 \pm 0.47 \,^{+0.02}_{-0.08}$ | $+0.28 \pm 0.26 \pm 0.13 \,^{+0.07}_{-0.05}$ $(0.6\sigma)$ |
| $\chi_{c0}K^+$ | $1.29 \pm 0.19 \pm 0.15 \,^{+0.12}_{-0.03}$ | $0.70 \pm 0.10 \pm 0.10 \,^{+0.06}_{-0.02}$ | $-0.14 \pm 0.15 \pm 0.03 \,^{+0.01}_{-0.05}$ $(0.5\sigma)$ |
| $\rho(770)^0K^+$ | $6.54 \pm 0.81 \pm 0.58 \,^{+0.69}_{-0.26}$ | $3.56 \pm 0.45 \pm 0.43 \,^{+0.38}_{-0.15}$ | $+0.44 \pm 0.10 \pm 0.04 \,^{+0.05}_{-0.13}$ $(3.7\sigma)$ |
| $\omega(782)K^+$ | $0.17 \pm 0.24 \pm 0.03 \,^{+0.05}_{-0.08}$ | $0.09 \pm 0.13 \pm 0.02 \,^{+0.03}_{-0.04}$ | — |
| $f_2(1270)K^+$ | $0.91 \pm 0.27 \pm 0.11 \,^{+0.24}_{-0.17}$ | $0.50 \pm 0.15 \pm 0.07 \,^{+0.13}_{-0.09}$ | $-0.85 \pm 0.22 \pm 0.13 \,^{+0.22}_{-0.02}$ $(3.5\sigma)$ |
| $B^0 \to K^+\pi^-\pi^0$ (total) | $102.3 \,^{+7.1}_{-4.0} \pm 4.1$ | $35.7 \,^{+2.6}_{-1.5} \pm 2.2$ | $-0.030 \,^{+0.045}_{-0.051} \pm 0.055$ |
| Non-resonant | $12.4 \pm 2.6 \,^{+1.3}_{-1.2}$ | $4.4 \pm 0.9 \pm 0.5$ | $+0.23 \,^{+0.19}_{-0.27} \,^{+0.11}_{-0.10}$ |
| $(K\pi)^{*+}_0\pi^-$ | $26.3 \,^{+3.1}_{-3.8} \,^{+2.1}_{-2.0} \pm 4.9$ | $9.4 \,^{+1.1}_{-1.3} \,^{+1.4}_{-1.1} \pm 1.8$ | $+0.17 \,^{+0.11}_{-0.16} \pm 0.09 \pm 0.20$ |
| $K^*(892)^+\pi^-$ | $11.8 \,^{+2.5}_{-1.5} \pm 0.6$ | $4.2 \,^{+0.9}_{-0.5} \pm 0.3$ | $-0.19 \,^{+0.20}_{-0.15} \pm 0.04$ |
| $(K\pi)^{*0}_0\pi^0$ | $24.3 \,^{+3.0}_{-2.6} \,^{+3.7}_{-3.0} \pm 6.7$ | $8.7 \,^{+1.1}_{-0.9} \,^{+1.8}_{-1.3} \pm 2.2$ | $-0.22 \pm 0.12 \,^{+0.13}_{-0.11} \pm 0.27$ |
| $K^*(892)^0\pi^0$ | $6.7 \,^{+1.3}_{-1.5} \,^{+0.7}_{-0.6}$ | $2.4 \pm 0.5 \pm 0.3$ | $-0.09 \,^{+0.21}_{-0.24} \pm 0.09$ |
| $\rho(770)^-K^+$ | $22.5 \,^{+2.2}_{-3.7} \pm 1.2$ | $8.0 \,^{+0.8}_{-1.3} \pm 0.6$ | $+0.11 \,^{+0.14}_{-0.15} \pm 0.07$ |

necessary to extract its decay property accurately.

The analysis is performed based on a 347.5 fb$^{-1}$ data sample containing $(383.2 \pm 4.2) \times 10^6$ $B\overline{B}$ pairs [9]. The isobar model that gives the best fit quality is listed in Table 1. Non-resonant contribution is modeled with a constant complex amplitude. For the $K\pi$ $S$-wave, referred as to $(K\pi)^{*0}_0$, and $f_0(980)$, parameterizations proposed by LASS [10] and Flatté [11] are used, respectively. Relativistic Breit-Wigner is used for the others.

Obtained results are listed in Table 1. We find evidence for direct $CP$ violation in $B^+ \to \rho(770)^0K^+$; the significance remains above $3\sigma$ with alternative models. Fit projections on the $\pi^+\pi^-$ invariant mass around $\rho(770)^0$ are shown in Fig. 2 $B^+$ and $B^-$ candidates separately. The sizable $\mathcal{A}_{CP}(\rho(770)^0K^+)$ is consistent with the SM prediction, unlike $\mathcal{A}_{CP}(K^+\pi^0)$. Significance of $\mathcal{A}_{CP}(f_2(1270)K^+)$ suffers from the large model uncertainty. No sizable $\mathcal{A}_{CP}$ is seen in the penguin-dominant decays of $B^+ \to K^*(892)^0\pi^+$, $(K\pi)^{*0}_0\pi^+$ and $K^*_2(1430)^0\pi^+$, which is consistent with the SM predictions.

Contributions of $f_2(1270)K^+$ and $f_X(1300)K^+$ are necessary to obtain a good fit, with $f_X(1300)$ being a scalar; the mass and width are measured to be $(1479 \pm 8)$ MeV/$c^2$ and $(80 \pm 19)$ MeV/$c^2$, respectively, which are consistent with those of $f_0(1500)$.

### 3.2. Decay of $B^0 \to K^+\pi^-\pi^0$

Dalitz plot analyses of $B \to K\pi\pi$ can provide magnitudes of and relative phases among $B \to K^*\pi$, which are of particular interest to give a constraint on the CKM parameters $(\overline{\rho}, \overline{\eta})$, or $\gamma$ if electroweak penguin contribution is negligible [12,13]. A Dalitz plot analysis of $B^0 \to K^+\pi^-\pi^0$ can provide such information for $B^0 \to K^{*0}\pi^0$ and $K^{*+}\pi^-$.

The analysis is performed based on a 210.6 fb$^{-1}$ data sample containing $(231.8 \pm 2.6) \times 10^6$ $B\overline{B}$ pairs [14]. The analysis is similar to that of $B^+ \to K^+\pi^-\pi^+$. For the $\rho^-$ line shapes, Gounaris-Sakurai parametrization [15] is used.

Obtained results are listed in Table 1. Fits found four solutions over which the results are averaged. The $B^0 \to K^*(892)^0\pi^0$ decay has been observed, for the first time, at $5.6\sigma$ sig-

Table 2
Results obtained in the analyses of $B \to PP$, $VP$ and $b_1 P$ [18,19,26]. The first and second errors are statistical and systematic, respectively; the latter is accounted in the evaluation of signal significance ($\mathcal{S}$). An upper limit on $\mathcal{B}$ at 90% confidence level is shown in the parenthesis for a mode which has not been observed yet. The $\mathcal{B}$ results are corrected for sub-decay branching fractions, where $\mathcal{B}(b_1 \to \omega\pi) = 1$ is assumed for $b_1$. The results are averaged over sub-decay channels where applicable.

| Mode | $\mathcal{S}$ [$\sigma$] | $\mathcal{B}$ [$10^{-6}$] | Ref. |
|---|---|---|---|
| $\eta K^0$ | 2.6 | $0.9\ ^{+\ 0.5}_{-\ 0.4} \pm 0.1$ ($< 1.6$) | [19] |
| $\eta\pi^0$ | 2.2 | $0.9 \pm 0.4 \pm 0.1$ ($< 1.5$) | [18] |
| $\eta'\pi^0$ | 3.1 | $0.9 \pm 0.4 \pm 0.1$ ($< 1.5$) | [18] |
| $\eta\eta$ | 2.4 | $0.8 \pm 0.4 \pm 0.1$ ($< 1.4$) | [19] |
| $\eta'\eta$ | 1.4 | $0.5 \pm 0.4 \pm 0.1$ ($< 1.2$) | [18] |
| $\eta'\eta'$ | 1.3 | $0.9\ ^{+\ 0.8}_{-\ 0.7} \pm 0.1$ ($< 2.1$) | [19] |
| $\eta\rho^+$ | 9.0 | $9.9 \pm 1.2 \pm 0.8$ | [18] |
| $\eta\phi$ | 1.7 | $0.22\ ^{+\ 0.19}_{-\ 0.15} \pm 0.01$ ($< 0.52$) | [19] |
| $\eta\omega$ | 3.5 | $1.0\ ^{+\ 0.4}_{-\ 0.3} \pm 0.1$ ($< 1.6$) | [19] |
| $\eta'\phi$ | 1.3 | $0.5 \pm 0.4 \pm 0.1$ ($< 1.2$) | [19] |
| $\eta'\omega$ | 3.1 | $1.0\ ^{+\ 0.5}_{-\ 0.4} \pm 0.1$ ($< 1.7$) | [19] |
| $\pi^0\omega$ | 0.3 | $0.07 \pm 0.26 \pm 0.02$ ($< 0.5$) | [18] |
| $b_1^+ K^0$ | 6.3 | $9.6 \pm 1.7 \pm 0.9$ | [26] |
| $b_1^0 K^0$ | 3.4 | $5.1 \pm 1.8 \pm 0.5$ ($< 7.8$) | [26] |
| $b_1^+ \pi^0$ | 1.6 | $1.8 \pm 0.9 \pm 0.2$ ($< 3.3$) | [26] |
| $b_1^0 \pi^0$ | 0.5 | $0.4 \pm 0.8 \pm 0.2$ ($< 1.9$) | [26] |

nificance taking into account the systematic uncertainty. We obtain $\mathcal{B}(K^*(892)^0\pi^0) = (3.6 \pm 0.7 \pm 0.4) \times 10^{-6}$ after correcting for the sub-decay branching fraction, which is assumed to be $\mathcal{B}(K^*(892)^0 \to K^+\pi^-) = 2/3$. No significant $\mathcal{A}_{CP}$ is seen.

Using the magnitudes and the relative phases obtained in this analysis and in a time-dependent Dalitz plot analysis of $B^0 \to K^0_S\pi^+\pi^-$ [16], a constraint on $(\overline{\rho}, \overline{\eta})$ is derived in Ref. [17]. Further improvement in the measurements would help to overconstrain the CKM parameters.

## 4. (QUASI-)TWO-BODY DECAYS

### 4.1. Decays with isoscalar mesons

Quite a few updates are made on searches for $B \to PP$ and $PV$ decays with isoscalar mesons. The analyses are performed for $B^+ \to \eta\rho^+$ and $B^0 \to \eta'\eta$, $\eta^{(\prime)}\pi^0$ and $\omega\pi^0$ based on a 418 fb$^{-1}$ data sample containing $(459 \pm 5) \times 10^6$ $B\overline{B}$ pairs [18]. For $B^0 \to \eta K^0$, $\eta^{(\prime)}\eta^{(\prime)}$, $\eta^{(\prime)}\phi$ and $\eta^{(\prime)}\omega$, a 423.5 fb$^{-1}$ data sample containing $(465 \pm 5) \times 10^6$ $B\overline{B}$ pairs is used [19]. An intermediate state particle is reconstructed from the most dominant decay channel only, except $\eta$ and $\eta'$ for which $\eta \to \gamma\gamma$ and $\pi^+\pi^-\pi^0$ and $\eta' \to \eta(\to \gamma\gamma)\pi^+\pi^-$ and $\rho^0\gamma$ are used, respectively.

Obtained results are listed in Table 2. The $B^+ \to \eta\rho^+$ decay is observed at $9\sigma$ significance, where $\mathcal{A}_{CP} = 0.13 \pm 0.11 \pm 0.02$ is obtained. Evidences are seen for $B^0 \to \eta'\pi^0$ and $\eta^{(\prime)}\omega$ at $3\sigma$ level. No signals are indicated for the others.

Theoretical predictions seem to generally agree with the measurements [19], but measurements show a pattern of $\mathcal{B}(\eta K^0) < \mathcal{B}(\eta K^+)$ [4,20,21] which are expected to be nearly equal [22]. Further improvement on the analysis of $B^0 \to \eta K^0$ seems necessary for a better understanding.

Contribution of tree amplitudes in $B^0 \to \eta' K^0$ and $\phi K^0$, which produce $\Delta S$, can be evaluated from the obtained $\mathcal{B}$ results. $B^0 \to \eta^{(\prime)}\pi^0$ and $\eta^{(\prime)}\eta^{(\prime)}$ can be used to constrain $\Delta S(\eta' K^0)$ [23,24] and $B^0 \to \pi^0\omega$, $\eta^{(\prime)}\omega$ and $\eta^{(\prime)}\phi$ for $\Delta S(\phi K^0)$ [23]. Derived constraints on $\Delta S$ are demonstrated in Ref. [25].

### 4.2. Decays of $B \to b_1 K^0$ and $b_1\pi^0$

New searches are performed for $B \to b_1 K^0_S$ and $b_1\pi^0$ based on a 424 fb$^{-1}$ data sample containing $(465 \pm 5) \times 10^6$ $B\overline{B}$ pairs [26]. The $b_1$ candidate is reconstructed from $b_1 \to \omega(\to \pi^+\pi^-\pi^0)\pi$.

Obtained results are listed in Table 2. The $B^+ \to b_1^+ K^0_S$ decay is observed at $6.3\sigma$ significance, where $\mathcal{A}_{CP} = -0.03 \pm 0.15 \pm 0.02$ is obtained. An evidence for $B^0 \to b_1^0 K^0$ is seen at $3.4\sigma$ significance. No signal is indicated for the final states involving $\pi^0$.

Possible deviations from theoretical predictions can be also seen in Further new or improved measurements would open more windows to probe new physics.

## 5. SUMMARY

Dalitz plot analyses of $B \to K^+\pi^-\pi^+$ and $K^+\pi^-\pi^0$ are updated. Evidence of direct $CP$ violation is seen in $B^+ \to \rho(770)^0 K^+$, which gives a useful input to the $\Delta\mathcal{A}_{CP}(K\pi)$ puzzle. The $B^0 \to K^*(892)^0\pi^0$ decay is observed for the first time. Amplitudes of $K^*\pi$ provide useful informa-

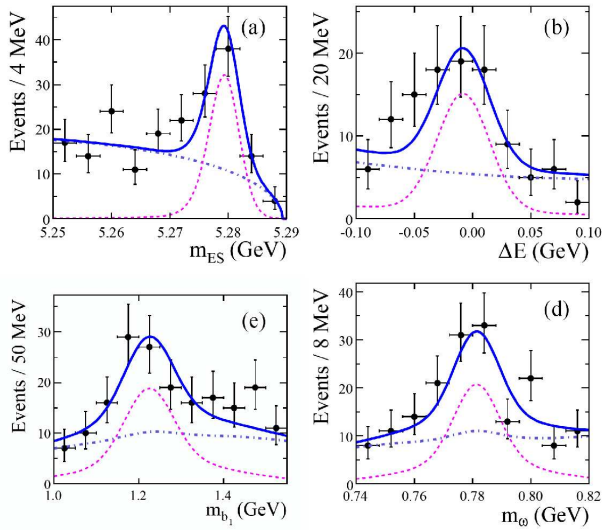


Figure 3. Fit projections for the $B^+ \to b_1^+ K_S^0$ candidates in signal-enhanced subsets [26]. Projections are made on $m_{\rm ES}$ (upper left), on $\Delta E$ (upper right), and on the invariant masses of $\pi^+\pi^-\pi^0\pi^+$ (lower left) and $\pi^+\pi^-\pi^0$ (lower right) in the regions of $b_1$ and $\omega$, respectively. Fit components are shown as the solid, dashed and dot-dashed curves for the total, signal and background, respectively; they are superimposed on the data points, shown with error bars.

tion to constrain the CKM parameters. Quite a few searches are performed for $B \to PP$ and $PV$ with isoscalar mesons, and for $B \to b_1 K^0$ and $b_1\pi^0$. Signals are observed for $B^+ \to \eta\rho^+$ and $b_1^+ K^0$. Evidences at $3\sigma$ significance level are seen for $B^0 \to \eta'\pi^0$, $\eta^{(\prime)}\omega$ and $b_1^0 K^0$. Obtained decay properties can be used to constrain $\Delta S$ or to open more windows to probe new physics. Charmless hadronic $B$ decays provide rich field to test the SM and to probe new physics.

## REFERENCES


1. N. Cabibbo, Phys. Rev. Lett. **10** (1963) 531; M. Kobayashi and T. Maskawa, Prog. Theor. Phys. **49** (1973) 652.
2. Belle Collaboration (S.-W. Lin *et al.*), Nature **452** (2008) 332.
3. BaBar Collaboration (B. Aubert *et al.*), Phys. Rev. Lett. **99** (2007) 021603; BaBar Collaboration (B. Aubert *et al.*), Phys. Rev. **D 76** (2007) 091102.
4. Heavy Flavor Averaging Group, http://www.slac.stanford.edu/xorg/hfag/.
5. Y. Gao, talk at this conference.
6. W. Kozanecki, Nucl. Instrum. Methods. Phys. Res., Sect. A **446** (2000) 59.
7. BaBar Collaboration (B. Aubert *et al.*), Nucl. Instrum. Methods. Phys. Res., Sect. A **479** (2002) 1.
8. BaBar Collaboration (B. Aubert *et al.*), Phys. Rev. Lett. **93** (2004) 231801.
9. BaBar Collaboration (B. Aubert *et al.*), Phys. Rev. **D 78** (2008) 012004.
10. LASS collaboration (D. Aston *et al.*), Nucl. Phys. **B 296** (1988) 493.
11. S.M. Flatté, Phys. Lett. **63** (1976) 224.
12. M. Ciuchini, M. Pierini and L. Silvestrini, Phys. Rev. **D 74** (2006) 051301(R).
13. M. Gronau, D. Pirjol, A. Soni and J. Zupan, Phys. Rev. **D 75** (2007) 014002.
14. BaBar Collaboration (B. Aubert *et al.*), Phys. Rev. **D 78** (2008) 052005.
15. G.J. Gounaris and J.J. Sakurai, Phys. Rev. Lett. $\mathcal{B}21$ (1968) 244.
16. BaBar Collaboration (B. Aubert *et al.*), arXiv:0708.2097 [hep-ex].
17. M. Gronau, D. Pirjol, A. Soni and J. Zupan, Phys. Rev. **D 77** (2008) 057504; Phys. Rev. **D 78** (2008) 017505.
18. BaBar Collaboration (B. Aubert *et al.*), Phys. Rev. **D 78** (2008) 011107(R).
19. W.T. Ford, arXiv:0810.0494 (2008).
20. BaBar Collaboration (B. Aubert *et al.*), Phys. Rev. **D 76** (2007) 031103(R).
21. Belle Collaboration (P. Chang *et al.*), Phys. Rev. **D 75** (2007) 071104(R).
22. A.R. Williamson and J. Zupan, Phys. Rev. **D 74** (2006) 014003.
23. Y. Grossman, Z. Ligeti, Y. Nir and H. Quinn, Phys. Rev. **D 68** (2003) 015004.
24. M. Gronau, J.L. Rosner and J. Zupan, Phys. Lett. **B 596** (2004) 107.
25. M. Gronau, J.L. Rosner and Z. Zupan, Phys. Rev. **D 74** (2006) 093003.
26. BaBar Collaboration (B. Aubert *et al.*), Phys. Rev. **D 78** (2008) 011104(R).
27. W. Wang, R.-H. Li and C.-D. Lü, arXiv:0806.2510 [hep-ph]